Landslides (2020) 17:1207–1216
DOI 10.1007/s10346-020-01351-4
Received: 15 August 2019
Accepted: 9 January 2020
Published online: 21 January 2020

Shufeng Tian · Ningsheng Chen · Hua Wu · Chengye Yang · Zheng Zhong · Mahfuzur Rahman

New insights into the occurrence of the Baige landslide along the Jinsha River in Tibet

Abstract The catastrophic Baige landslide occurred on October 10, 2018 in the Tibet Autonomous Region, China, and formed a barrier lake with a direct economic loss of 6.8 billion RMB (~ 963.5 million USD). After the landslide, field investigations were conducted both to support emergency operations and to understand the failure mechanism immediately after the landslide. Detailed field surveys, borehole exploration, discharge measurements, laboratory experiments, and meteorological analyses were employed in this study to explore the mechanisms underlying the Baige landslide. A key influence from the water source in Bogong Gully on the Baige landslide formation was newly found. The results show that the underground of the slope comprises extremely weathered serpentinite, and fresh rock has not yet been revealed in boreholes. The seepage outlets are 450–550 m higher than the Jinsha River and ~ 118 m lower than the bed of Bogong Gully. Water flow in the channel of Bogong Gully is strongly infiltrated, with a flow loss of 62.6%. Seepage into the Bogong Gully, along with the landslide, caused by the local geological structure and lithology, accelerated the extreme weathering of rock masses and promoted landslide formation. Furthermore, extreme annual rainfall also contributed to the occurrence of the Baige landslide by increasing the discharge of the Bogong Gully. Further risk management measures in this area should include increasing the depth of geological explorations and the construction of drainage systems.

Keywords Baige landslide · Slope seepage · Tectonics · Groundwater · Rainfall · Risk management

Introduction

The Baige landslide was a massive landslide that caused disaster by blocking the Jinsha River. Two landslides occurred at the same place in Baige Village on October 10, 2018 and November 3, 2018, along the border between Sichuan Province and the Tibet Autonomous Region in China and on the right bank of the Jinsha River, with total volumes of 22 million m^3 and 3.7 million m^3, respectively (Fan et al. 2019, Liang et al. 2019, Xu et al. 2019, Zhang et al. 2019). The residual deposit of the first landslide in the riverbed caused the second landslide to block the river, forming a barrier lake. The barrier lake seriously threatened local hydropower stations and the safety of residents along the river. The upstream inundation distance was > 20 km, where hundreds of houses in the villages of Baige and Ningba in Boluo County were submerged, and 17,307 people were evacuated. The barrier lake was discharged through manual intervention on November 13, 2018, and the resultant dam burst collapsed 8051 houses downstream, damaged 33 km^2 of agricultural lands, and 632.12 km of road in Yunnan Province. The direct economic loss was 6.8 billion RMB (~ 963.5 million USD). In recent years, the Jinsha River has been extensively developed for hydroelectric power generation, and the government plans to construct ~ 27 large hydropower stations along the Jinsha River. Therefore, understanding the essential cause and generative characteristics of these landslides is extremely important.

After the Baige landslide, many researchers studied the landslide characteristics and deformation history through initial investigations and multi-temporal satellite images (e.g., Deng et al. 2019, Fan et al. 2019, Xu et al. 2019). Ouyang et al. (2019) studied the initial deformation observed via optical remote sensing images and interferometric synthetic aperture radar (InSAR) and assessed the dynamic characteristics using numerical simulations. Wu et al. (2019) studied the early warning system applied in the Baige landslide, while Yang et al. (2019) detected the slope movement of the Baige landslide from November of 2015 to August of 2018 by analyzing Sentinel-2 images. Zhang et al. (2019) studied the source characteristics and dynamics of the October 2018 Baige landslide by analyzing broadband seismograms. However, Liang et al. (2019) noted that it remains unclear why the landslides occurred. In this study, the fundamental cause of landslide formation was analyzed to better understand the occurrence of the Baige landslide. Determining the causal mechanism is a key for predicting and mitigating the hazards of landslides, including the formation of landslide-dammed lakes.

The towns and villages upstream of the Jinsha River remain in a state of disaster relief, and the residents, who had been evacuated, have been unable to return. Efforts are being made to reduce future disaster risks by dredging deposits and reducing the potential landslide volume. Shortly after the occurrence of the Baige landslide, the road to the landslide site was damaged by the landslide-dammed lake. Due to limited access and the lack of investigative depth soon after the disaster, the generative characteristics and mechanism of the Baige landslide remain unclear. Therefore, risk management and control methods informed by the disaster have not yet been resolved. It is worrying that subsequent landslides will further increase the disaster risk of damming the river. Thus, we aimed to discover the essential generative cause of the Baige landslide through detailed field investigations and geological analyses, while also noting the long-term tectonic and extreme climatic drivers of the Baige landslide via their effects on the evolution and runoff of the Bogong Gully. It is expected that the results of this study will provide theoretical support for the improvement of disaster prevention and risk mitigation measures in communities along the Jinsha River.

Regional setting

Geographic location and geomorphological characteristics

On the evening of October 10, 2018, at 22:05:36 (Beijing time, UTC+ 8; all the time in this article are converted to UTC+ 8), the first large-scale landslide occurred along the right bank of the Jinsha River at the border of Baiyu County in Sichuan Province and Jiangda County in the Tibet Autonomous Region (31°4′56.41″ N, 98°42′17.98″ E). The first landslide had a volume of 22×10^6 m^3,

which blocked the mainstream of the Jinsha River and impounded a 290-million-m^3 lake. The lake was naturally discharged at 17:30 on October 12, 2018. Based on the residual deposits from the first landslide, the Jinsha River was severely blocked by the second landslide, which had a volume of 3.7×10^6 m^3 and occurred at 17:40 on November 3, 2018. The second landslide impounded a 105×10^6-m^3 lake, and the barrier lake was successfully discharged through manual intervention on November 13th.

The Baige landslide is located on a ridge of a concave bank of the Jinsha River. The foot of the landslide has historically been washed and eroded by the Jinsha River. As shown in Fig. 1, the landslide area is ~ 0.86 km^2, with a sliding direction of 105°. The elevation varies from 2890 to 3720 m, with a relative height difference of ~ 830 m. The landslide has an extensive history of deformation, which illustrates that it is a creeping landslide. The slope began to deform in 1966, but it was not obvious. The maximum horizontal displacement since 2011 reached 47 m increasing by 26 m between 2017 and 2018 (Fan et al. 2019, Xu et al. 2019).

The vegetative cover in the study area is relatively dense, but the surface of the slope is somewhat bare relative to the surrounding mountains, while the exposed area of weathered bedrock and soil is relatively large. According to Google Earth v. 7.3 images, there are no obvious channels on the surface of the slope, and the density of the groove is small. The Bogong Gully, with a drainage area of 23.2 km^2, is located on the western side of the Baige landslide. The main channel of this gully rotates ~ 89° at the ridge of the mountain upon which the Baige landslide is located.

Geological and hydrological characteristics

The study area belongs to a tectonically eroded area, with a cold and frozen weathered landform, and a continental monsoon climate. The mean annual precipitation and temperature are 626 mm and 8 °C, respectively (Xu et al. 2019). Factors, such as regional tectonics and groundwater conditions, lead to the development of joints and fissures, which result in the poor integrity and mechanical properties of rock masses. The exposed lithology in the study area is mainly a Proterozoic gray gneiss (P_tXn^2) and a gray-green serpentinite (ϕ_{w4}) from the Variscan (Hercynian) Orogeny. The attitude (strike and dip) of the gneiss is 238°∠67°.

On the western side of the landslide, the Bolo-muxie thrust fault traverses the Bogong Gully and crosscuts the Variscan serpentinite and overlying Triassic strata, illustrating that the fault formed after the Late Triassic. Feng et al. (2019) revealed through field investigations that there may be a fault (red line in Fig. 2) that serves as the unconformable contact between the serpentinite and gneiss.

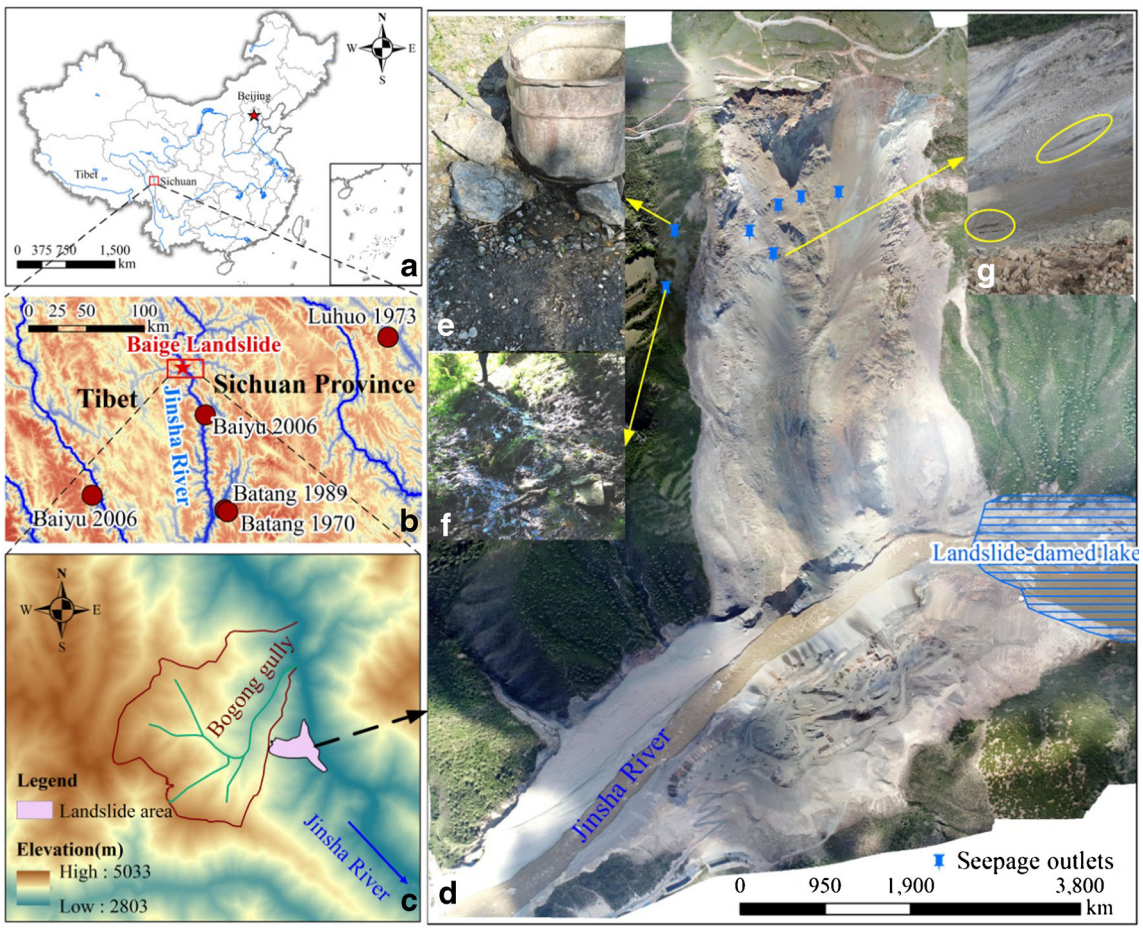

Fig. 1 Location and geographic background of the study area. **a** Baige landslide at the border of the Sichuan Province and Tibet Autonomous Region. **b** Earthquakes near the Baige landslide and landslide location. **c** Bogong Gully at the back of the Baige landslide. **d** Orthoimage of the Baige landslide via unmanned aerial vehicle (UAV), and **e–g** seepage outlets on the slope

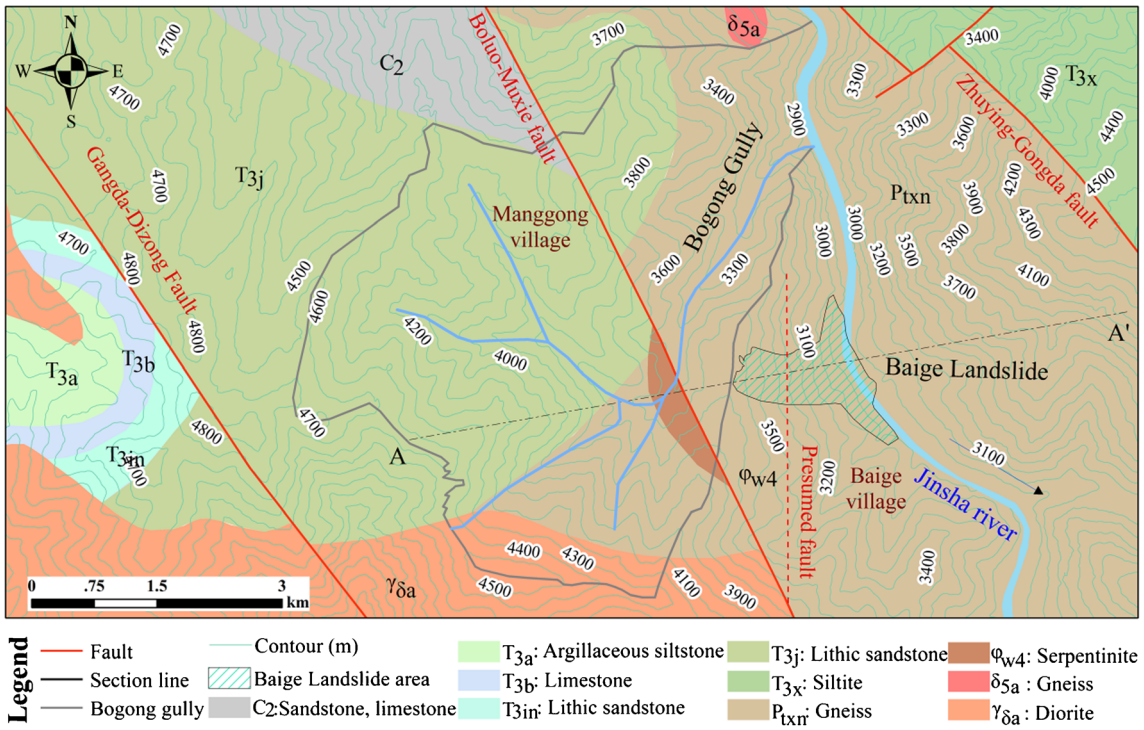

Fig. 2 Geological map of the study area

Based on interviews of local residents, the main channel of the Bogong Gully has water year-round, with the discharge being the largest in summer, and there is ice in the channel during winter (starting from October). Tectonic folding is developed on the

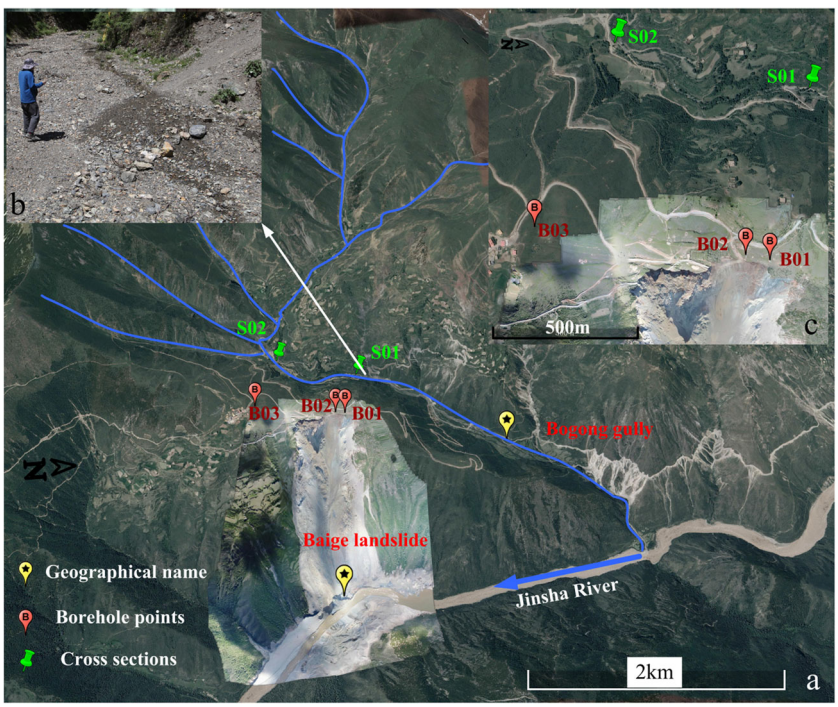

Fig. 3 Geomorphology of the Baige landslide and on-site surveys in the study area. **a** Red labels (B01, B02, and B03) are three engineering geological boreholes conducted by Sichuan bureau of geology & mineral resources, and green labels (S01 and S02) are the positions of flow measurements in the main channel of the Bogong Gully. **b** The seepage phenomenon in Bogong Gully. **c** The vertical view of B01, B02, B03, S01, and S02 in the study area

Stratum	Th./m	Elev./m	Cross section	Description
Q_l^{al}	4.00	3723.00		Yellow diluvium, poor integrity, including gravel
$P_t xn$	0.72	3722.28		Gray gneiss, silky luster, broken structure
	3.76	3718.52		Brown gneiss, silky luster, broken structure
φ_{w4}	3.20	3715.32		Gray-green serpentinite, broken structure, iron stain
	3.52	3711.80		Gray serpentinite, fragmented structure
	0.80	3711.00		Gray serpentinite, relatively complete structure
	9.00	3702.00		Gray severely weathered serpentinite including complete structure
	1.00	3701.00		Gray serpentinite, fragmented structure
	7.00	3694.00		Gray extremely weathered serpentinite
	3.70	3690.30		Gray serpentinite, fragmented structure
	3.30	3687.00		Gray extremely weathered serpentinite
	7.00	3680.00		Gray serpentinite, extremely fragmented structure, including weathered serpentinite
	17.00	3673.00		Grey-green extremely weathered serpentinite

Fig. 4 Soil profile at borehole B02

western side of the study area, further demonstrating that the Baige landslide occurred in a highly tectonically active region. There have been many earthquakes in this area since 1870. For example, as shown in Fig. 1b, the Batang earthquakes in 1870 and 1989, the Luhuo earthquake in 1973, the Baiyu earthquake in 2006 in Sichuan Province, and the 2013 Changdu earthquake in the Tibet Autonomous Region were not far from the study area. However, local residents have not felt any strong earthquakes, according to the on-site interviews.

In as early as 1988, the China Geological Survey reported that the groundwater resources in the study area are highly abundant, and mainly includes bedrock fissure water. Their report indicates that the spring water is exposed in the vicinity of some major fault zones, and there are significant fluctuations in groundwater levels with crustal uplift (Geological Survey Report of the People's Republic of China, 1988). The rock mass structure in this area is broken, and the fractured rock mass were important preconditions for the groundwater

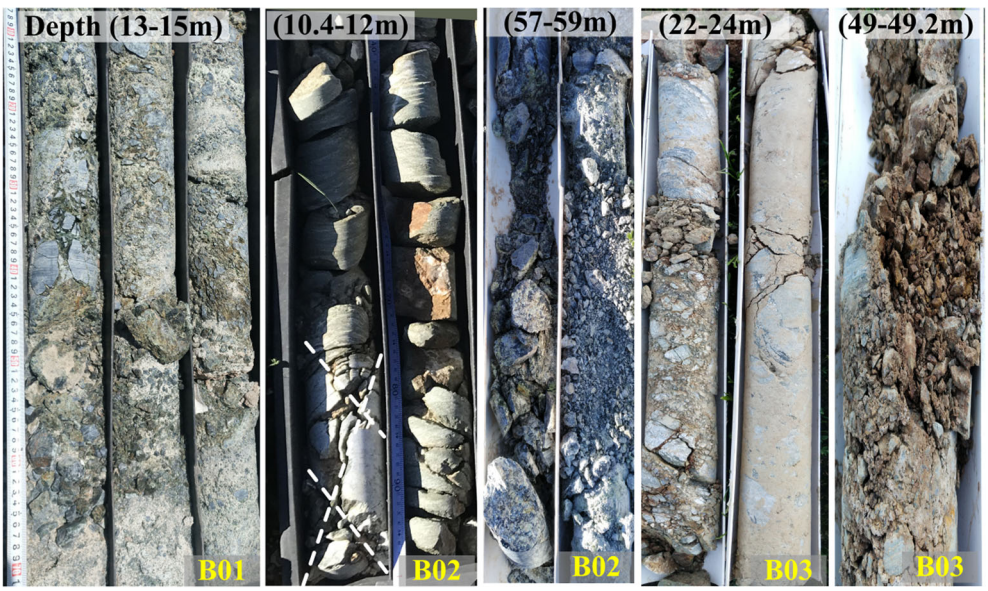

Fig. 5 Photograph of cores in boreholes B01, B02, and B03 showing the fractured and strongly weathered rock mass deep with the slope

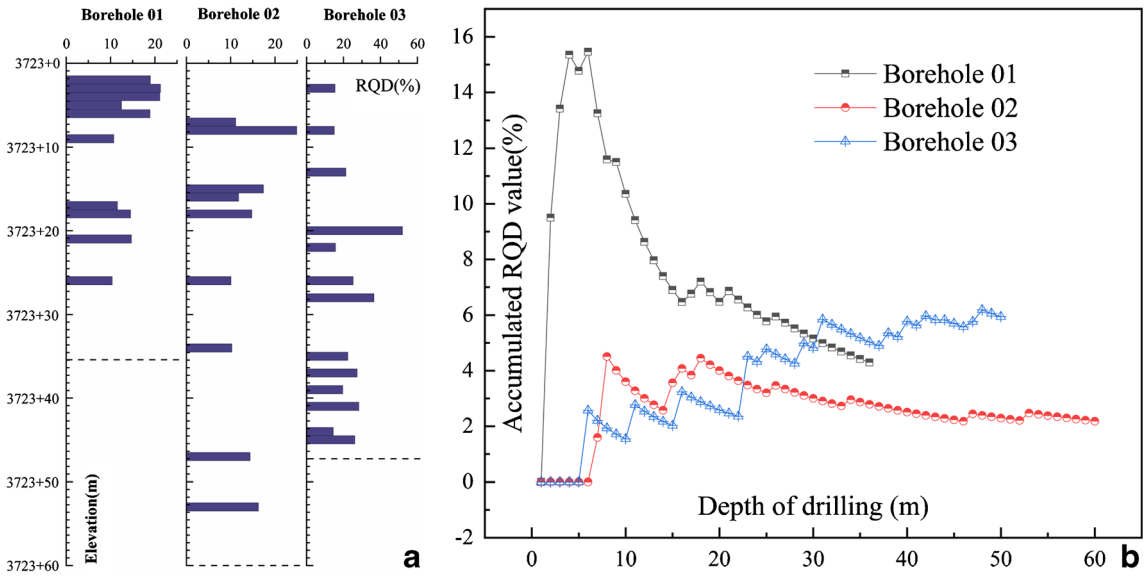

Fig. 6 Relationships between borehole depth, Rock Quality Designation (RQD) value, and accumulated RQD value. **a** Relationship between borehole depth and RQD value, the dotted line represents the depth of the borehole. **b** Relationship between borehole depth and accumulated RQD value

seepage (Li et al. 2008). Two joints are oriented at 65°∠56° and 120°∠37°.

Causal analysis of the Baige landslide

Water was the key factor controlling the occurrence of the Baige landslide. Under the impact of locally deformed and weathered geological structures, a metamorphic lithology, and extreme precipitation, water in the Bogong Gully, a branch of the Jinsha River with a catchment area of 23.2km^2, refilled the long-term seepage within the slope of the Baige landslide. The borehole revealed that the integrity of rock mass along the depth of the borehole is of poor condition. The strength of the serpentinite inside of the slope was drastically reduced during long-term seepage, which drove landslide formation. The strong weathering caused by seepage within the slope and the seepage replenishment from the Bogong Gully on the back side of the landslide provided the basic conditions necessary for the occurrence of the Baige landslide, while the extreme climatic conditions provided the necessary driver. Additionally, the potential slip mass near the Baige landslide still exists, and it should be further controlled based on the causes of the landslide. The location of the field survey and the spatial relationship between the Baige landslide, Bogong Gully, and Jinsha River are shown in Fig. 3.

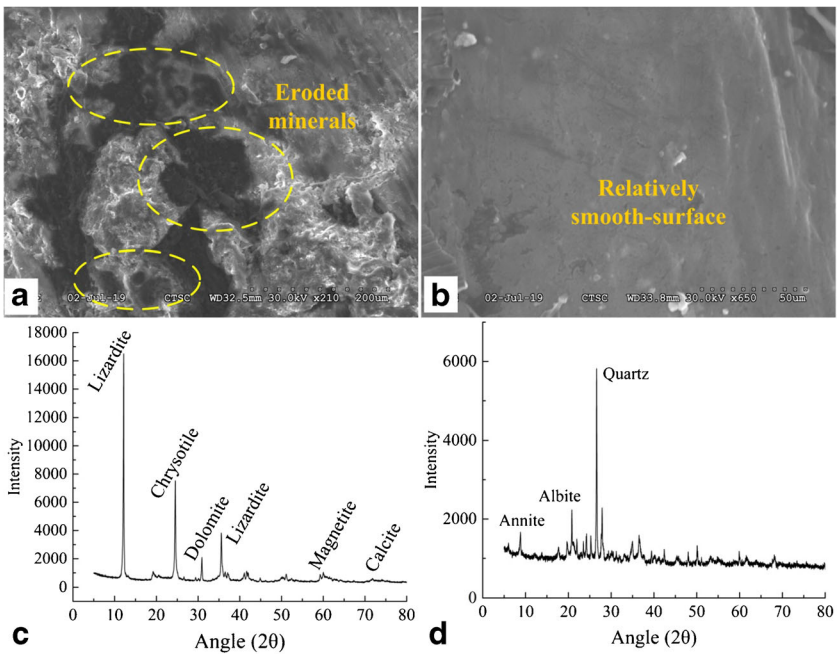

Fig. 7 Surface images of **a** weathered and **b** fresh rock under an S-3000N scanning electron microscope; eroded minerals are distributed in **a** but are absent from **b**. X-ray diffraction analytical results of **c** the rock and **d** rock weathering products at a depth of 17 m in borehole B03

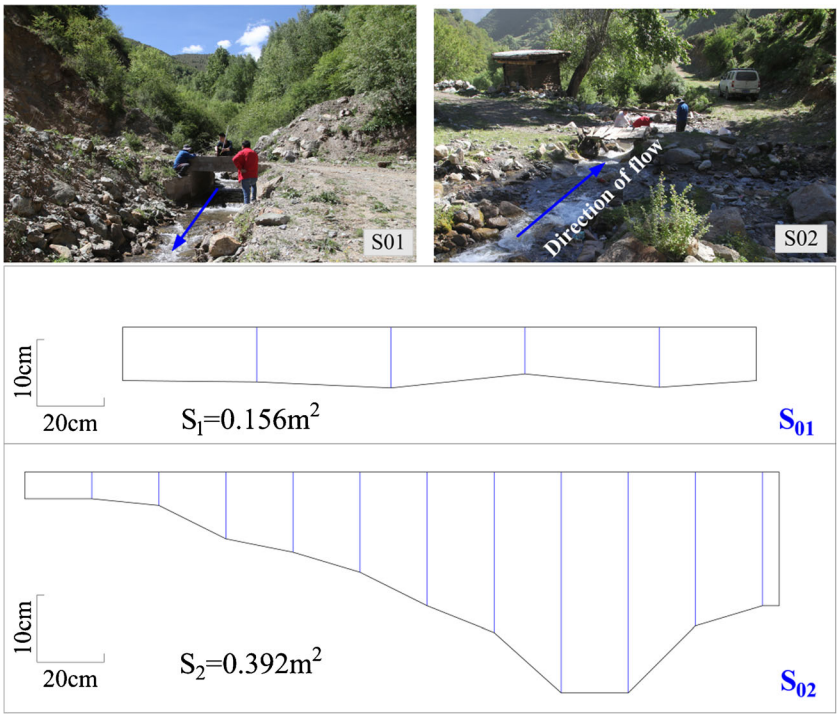

Fig. 8 Field survey (S01 and S02 in Fig. 3) and cross-sectional morphology in the Bogong Gully

Strongly weathered rock mass and groundwater conditions inside the landslide slope

Groundwater conditions in the study area are well-developed, and the long-term internal seepage into the slope leads to strong weathering of the rock mass, providing a conditioning factor for the occurrence of landslides. On-site investigations revealed that there are many seepage outlets on the surface of the slope since the Baige landslides occurred. As shown in Fig. 1c, these outlets are distributed along an elevational band of 3280–3450 m. The location of the two seepage outlets (Fig. 1d and e) measured on the slope are 31°4′43.4267″ N, 98°42′8.8055″ E (at 3434 m) and 31°4′43.3443″ N, 98°42′19.8193″ E (at 3282 m).

The concentrated distribution of houses and farmland on the slope further illustrates that the groundwater in this area is relatively abundant. Figure 4 shows a soil profile at borehole (site B02) indicating that the degree of fragmentation and weathering of the rock mass within the slope increases as the depth increases. The existing boreholes (B01, B02, and B03) revealed that the thickness of the weathered and fractured rock mass is > 60 m and notably includes highly weathered and low-integrity serpentinite (Fig. 5), which is associated with the active tectonics of the study area. The tectonic extrusion of a reverse fault caused fracturing of the rock mass inside of the slope.

A Rock Quality Designation (RQD) value was used in this study to evaluate the quality of the rock mass. This method is widely employed by engineering geologists (Deere et al. 1967, Ietto et al. 2017). The RQD values of the B01, B02, and B03 in the same soil profile show that the points with an RQD value of 0% occur intermittently, and these points are concentrated in the elevations of 3711–3714 m, 3698–3700 m, 3690 m–3694 m (Fig. 6a. This phenomenon may be caused by the fluctuation of the incision velocity in Bogong Gully. The accumulated RQD value was used to better show the relationship between the drill depth and the fracturing of the rock mass (Cui et al. 2018). The accumulated RQD values of the three boreholes at the top of the slope revealed that the rock quality first increases and then decreases with borehole depth, especially in B01 and B02. The accumulated RQD value of B01 is higher than those of B02 and B03 at a depth of 10 m, while the value of B03 (7%) is higher than those of B01 and B02 at a depth greater than 40 m,

Table 1 Calculation discharge of the Bogong Gully

No.	Location	Buoy distance (m)	Time(s)	Velocity(m/s)	Cross-sectional area(m^2)	Discharge(m^3/s)
S01	N 31°5′5.95″ E 98°41′26.98″; H = 3457 m	6.00	8.47	0.708	0.156	0.110
S02	N 31°4′46.71″; E 98°41′23.47″; H = 3552 m	6.00	8.00	0.750	0.392	0.294

Fig. 9 Roundness of soil samples revealed by sieving experiments. The top is of soil sample #1 and the bottom is of soil sample #2; the white stippled circle is the sampling position, and the orange solid circle is a sub-rounded grain

showing that the integrity of the rock mass is extremely poor (Fig. 6b).

Figure 7 a and b show the images of weathered and fresh sections of a rock sample obtained using an S-3000N scanning electron microscope (Hitachi Ltd., Japan). It was found that the surface of the fresh section was smooth, while that of the weathered section was rough and contained many holes. These holes were formed by the reaction between the clay minerals in the rock mass and the groundwater, which further illustrates the effects of long-term water–rock interactions inside of the slope. Additionally, X-ray diffraction (XRD) analyses revealed the mineral composition of the rock mass within the slope of the Baige landslide (Fig. 7c and d); 49% lizardite (H, Mg, O, and Si), 39% chrysotile (H, Mg, O, and Si), 9% dolomite (C, Ca, Mg, and O), 3% magnetite, and 1% calcite were found in the serpentinite. The compositions of the weathered soils at a depth of 17 m below the surface was 51% quartz (Si and O), 45% albite (Si and Ca), and 5% annite (Fe, O, and Si). The grain size of the quartz at a depth of 17 m below the surface was small, and the properties of the annite were similar to those of the clay minerals. These secondary minerals were formed in fissures by siliceous materials, which are the weathering products of serpentinite. These findings also indicate that the serpentinite in this area is strongly weathered under the action of intense groundwater activity.

Flow loss and the evolution of the Bogong Gully

The drainage area of the Bogong Gully is 23.2 m^2, and the length of the main channel is 8.55 km. The gully converges into the Jinsha River on the northern side of the Baige landslide. The discharges of two representative cross-sections (So1 and So2) along the back of the Baige landslide were calculated using a morphological surveying method in which the discharge is the product of the velocity and the cross-sectional area. The shape of the cross-section was obtained by field measurements, and the flow velocity was obtained by measuring the time over which a buoy passed a certain distance (Fig. 8). The calculated flow results are shown in Table 1.

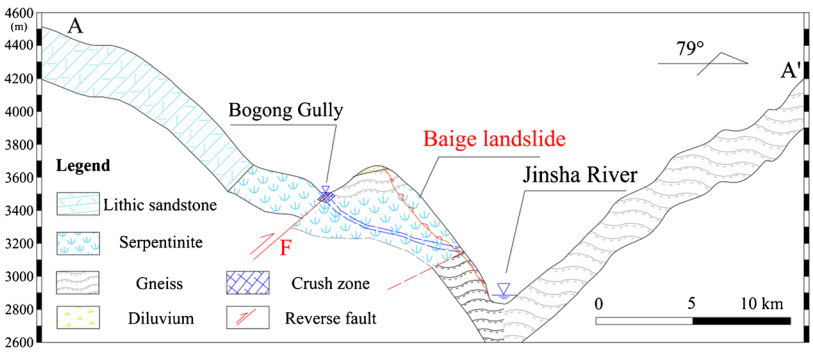

Fig. 10 Geological profile through the line A–A′ shown in Fig. 2. The stippled line is speculated fault

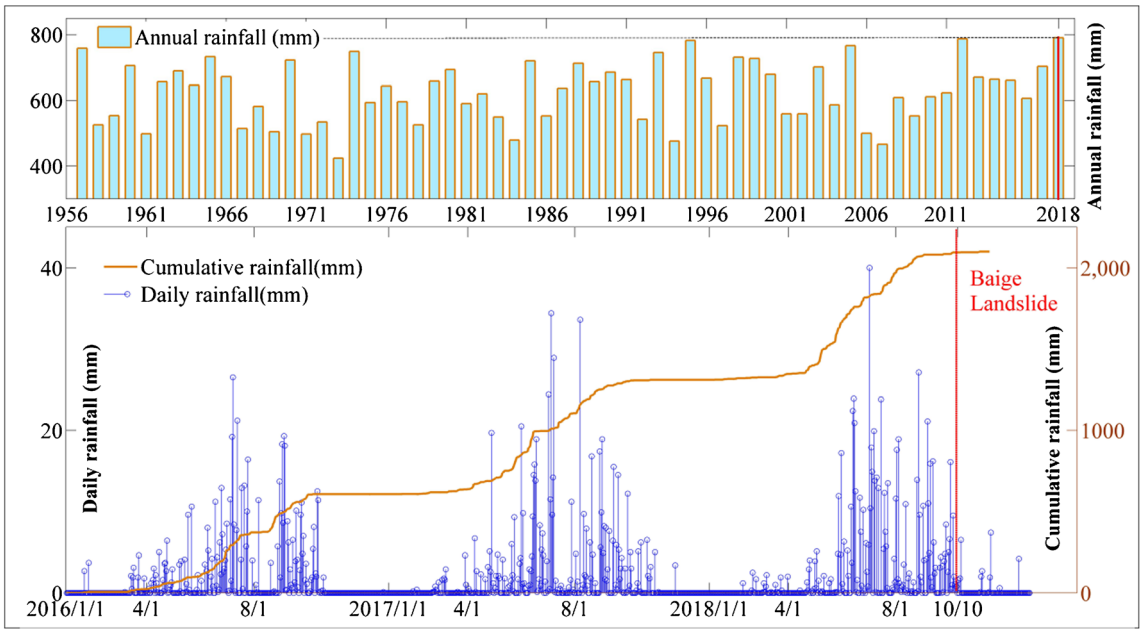

Fig. 11 Rainfall from the Dege County Meteorological Station near the study area from 1957 to 2018. The upper part is the annual rainfall from 1957 to 2018, and the lower part is the daily and accumulated daily rainfalls from 2016 until landslide occurrence

It was found that 62.6% of the water in the 680-m channel from S02 to S01 was involved in infiltration under the current runoff conditions from upstream to downstream. Additionally, the channel elevation of the Bogong Gully through the ridge of the Baige landslide ranges from 3453 to 3624 m, and the elevation of the seepage outlets on the surface ranges from 3280 to 3450 m. Thus, the elevation of the Bogong Gully is ~ 344–174 m higher than the seepage outlets on the slope surface.

A soil sample (#1) was taken from borehole B02 at a depth of 3.4 m, and another (#2) was taken from the top of the slope. We performed soil sieving experiments, and the results showed that both soil samples (#1 and #2) contain alluvial deposits with highly sub-rounded grains (Fig. 9). The particle sizes of sub-rounded grains in soil sample #1 are < 10 mm, and sub-rounded grains 10 mm in size accounted for only 10% of sample #1. Meanwhile, 20-mm sub-rounded grains in soil sample #2 were distributed across the sieve tray accounted for 30% of the sample. These findings indicate that the top of the slope of the Baige landslide has been eroded by the Bogong Gully, and that the hydrodynamic conditions have been gradually enhanced with the accumulation of alluvium. Therefore, the height of the bed in the Bogong Gully is historically consistent with the top of the Baige landslide, and the channel diversion and incision of the Bogong Gully resulted in the water level in the main channel drawing increasingly closer to the broken serpentinite within the slope.

The geological structure of the study area was analyzed according to the A–A' profile shown in Fig. 2, and its longitudinal profile is shown in Fig. 10. A SW-oriented reverse fault is developed on the western side of the Baige landslide, and the fault traverses the channel bed of the Bogong Gully. The Bogong Gully is located on the hanging wall of the fault, and the deep-seated serpentinite intruded prior to being seated on the landslide side in the footwall. In the process of uplifting, the fault zone became extremely broken, and the serpentinite on the hanging wall was gradually emplaced at the same level as the gneiss of the footwall. The erosion resistance of gneiss is greater than that of serpentinite, which led to the diversion of the Bogong Gully and the channel geomorphology being sharply turned 89° at the intersection of the serpentinite and fault.

Continuous incising of the Bogong Gully bed has resulted in the elevation of the serpentinite zone in the footwall being similar to that of the channel bed, which promotes seepage into the slope. Due to the high permeability of the fractured and weathered rocks, the serpentinite whole rock mass inside of the Baige landslide began to experience high-intensity infiltration. Moreover, the strata under the serpentinite are composed of gneiss, which is an impermeable layer, and thus, the water percolates along the unconformable contact between the serpentinite and the gneiss layer.

Extreme annual rainfall and potential future risks

Extreme weather prompted the occurrence of the Baige landslide, and the potential for future landslides exists. Therefore, fundamental risk management measures must be taken based on the generative mechanisms outlined in this study. A sudden increase in extreme annual rainfall events drove the occurrence of the Baige landslide. Existing meteorological data show that the Dege County Meteorological Station is the closest station with detailed data on the study area. The elevation of the station is similar to the top of the Baige landslide and the Bogong Gully. Therefore, the rainfall trends recorded at this meteorological station are essentially the same as in the study area.

The Baige landslide occurred at the end of the rainy season on October 10, 2018. However, there was no rain on that day. In October, the maximum daily rainfall was 16.1 mm/day, which is very common in the area. For example, there were 5 rainfall events that exceeded volumes of 16.1 mm/day in August and September of

Fig. 12 Tensile cracks on the slope after the Baige landslide

2018. Thus, the daily rainfall in October did not immediately lead to the occurrence of landslides. However, rainfall data from 1957 to 2018 show that the annual rainfall in 2018 was 790.4 mm, having reached a low-frequency rainfall, with a frequency of at least < 62 years. Also, the research suggests that daily rainfall did not directly trigger the Baige landslide, while the annual rainfall affected the strength and stability of the rock mass by increasing the infiltration volume caused by the increased discharge of the Bogong Gully. The rainfall characteristics and a hysteresis effect between the heavy daily rainfall and the timing of landslide are shown in Fig. 11.

At present, there is a potentially high landslide risk on the slope on the southern side of the Baige landslide. A number of cracks formed on the top of the slope after the Baige landslide (Fig. 12), and borehole B03 shows that the rock mass is strongly weathered. The groundwater remains active in the areas where no landslide had occurred on the southern end of the Baige landslide. Efforts are currently being made to reduce the disaster risk by dredging deposits and reducing the potential landslide volume. However, due to the limitations imposed by limited accessibility and the low geological exploration depth, the generative characteristics of the Baige landslide have not been fully clarified. Additionally, current emergency disposal methods following landslides have not resolved the fundamental problems facing this region, and the risks are likely to remain relatively high under the predicted extreme conditions in the future.

Conclusions

The Baige landslide was triggered by extreme climatic conditions and long-term seepage from Bogong Gully caused by regional tectonic activities. The seepage inside of the slope and the fractured rock mass were important preconditions for the occurrence of the Baige landslide, especially as the scale of seepage was amplified by the convergence of the Bogong Gully. Analyses of the roundness of the deposits at the top of the slope and of boreholes showed that regional tectonic activities not only break the rock mass but also change the channel geomorphology of the Bogong Gully. The main channel direction of the gully turns ~ 89° behind the mountain, and this rotation is jointly controlled by the faults and lithology of the study area. This geomorphology renders the Bogong Gully as an amplifier for the water source of the seepage within the slope, leading to an increase in seepage that is conducive to the occurrence of landslides.

Increased seepage caused by extreme precipitation triggered the Baige landslide. Although there was no rainfall during the landslide, the annual rainfall in the study area reached the maximum recorded in 2018. The daily rainfall on July 2, 2018 was the highest in recorded history. Thus, the Baige landslide was not directly triggered by rainfall but rather by the increased seepage caused by the extreme annual rainfall. Rainfall does not immediately lead to an increase in seepage. Therefore, there is a time lag between rainfall events and landslide event, which may explain the difficulty in coupling rainfall and landslides. Increasing rainfall promotes the discharge of seepage inside the slope, enhancing water–rock interactions, and reducing the strength of the rock mass.

The potential risk posed by the slope near the Baige landslide has not been eliminated, and the risk is likely to remain high in the future. Moreover, a series of tensile cracks generated at the top of the slope after the Baige landslide will lead to increased seepage at the top of the slope, further impacting groundwater activities. Thus, additional drainage measures and deep explorations must be implemented on the basis of existing prevention and control measures.

Funding information

This study was financially supported by the National Natural Science Foundation of China (Grant Nos. 41861134008 and 41671112), and the Key R&D Projects of Sichuan Science and Technology Project (Grant No. 18ZDYF0329). All financial supports are greatly appreciated.

References

Cui SH, Pei XJ, Huang RQ (2018) Effects of geological and tectonic characteristics on the earthquake-triggered daguangbao landslide, China. Landslides 15(4):649–667. https://doi.org/10.1007/s10346-017-0899-3

Deere DU, Hendron AJ, Patton FD, Cording EJ (1967) Design of surface and near-surface construction in rock. In: Fairhurst C (ed) Failure and breakage of rock. Society of Mining Engineers of AIME, New York, pp 237–302

Deng JH, Gao YJ, Yu ZQ, Xie HP (2019) Analysis on the formation mechanism and process of baige landslides damming the upper reach of Jinsha River, China. ADVANCED ENGINEERING SCIENCES 51(1):9–16. https://doi.org/10.15961/j.jsuese.201801438

Fan XM, Xu Q, Alonso-Rodriguez A, Subramanian SS, Li WL, Zheng G, Dong X, Huang R (2019) Successive landsliding and damming of the Jinsha River in eastern Tibet, China: prime investigation, early warning, and emergency response. Landslides 16(5):1003–1020. https://doi.org/10.1007/s10346-019-01159-x

Feng WK, Zhang GQ, Bai HL, Zhou YL, Xu Q, Zheng G (2019) A preliminary analysis of the formation mechanism and development tendency of the huge baige landslide in Jinsha River on October 11, 2018. J Eng Geol 27(2):415–425. https://doi.org/10.13544/j.cnki.jeg.2018-392

Geological Survey Report of the People's Republic of China, 1988, Tibet Autonomous Region Geology and Minerals Bureau. (In Chinese)

Ietto F, Perri F, Cella F (2017) Weathering characterization for landslides modeling in granitoid rock masses of the Capo Vaticano promontory (Calabria, Italy). Landslides 15(1):43–62. https://doi.org/10.1007/s10346-017-0860-5

Li P, Lu W, Long Y, Yang Z, Li J (2008) Seepage analysis in a fractured rock mass: the upper reservoir of Pushihe Pumped-Storage Power Station in China. Eng Geol 97:53–62. https://doi.org/10.1016/j.enggeo.2007.12.005

Liang GL, Wang Z, Zhang GW, Wu LL (2019) Two huge landslides that took place in quick succession within a month at the same location of jinsha river. Landslides 16(5):1059–1062. https://doi.org/10.1007/s10346-019-01165-z

Ouyang CJ, An HC, Zhou S, Wang ZW, Su PC, Wang DP, Cheng DQ, She JX (2019) Insights from the failure and dynamic characteristics of two sequential landslides at Baige village along the Jinsha River, China. Landslides 16(7):1397–1414. https://doi.org/10.1007/s10346-019-01177-9

Wu YB, Niu RQ, Lu Z (2019) A fast monitor and real time early warning system for landslides in the Baige landslide damming event, Tibet, China. Natural Hazards and Earth System Sciences Discussions:1–20. https://doi.org/10.5194/nhess-2019-48

Xu Q, Zheng G, Li WL, He CY, Dong XJ, Guo C, Feng WK (2019) Study on successive landslide damming events of Jinsha River in Baige village on Octorber 11 and November 3, 2018. Journal of Engineering Geology 26(6):1534–1551. https://doi.org/10.13544/j.cnki.jeg.2018-406

Yang WT, Wang YQ, Sun S, Wang YJ, Ma C (2019) Using sentinel-2 time series to detect slope movement before the Jinsha River landslide. Landslides 16(7):1313–1324. https://doi.org/10.1007/s10346-019-01178-8

Zhang Z, He S, Liu W, Liang H, Yan SX, Deng Y, Bai XQ, Chen Z (2019) Source characteristics and dynamics of the October 2018 Baige landslide revealed by broadband seismograms. Landslides 16(4):777–785. https://doi.org/10.1007/s10346-019-01145-3

S. Tian · N. Chen · M. Rahman
Key Lab of Mountain Hazards and Surface Processes, Institute of Mountain Hazards and Environment,
Chinese Academy of Sciences,
Chengdu, 610041, China

S. Tian · M. Rahman
University of Chinese Academy of Sciences,
Beijing, 100049, China

N. Chen (✉) · H. Wu · C. Yang
Joint Laboratory of Plateau Surface Remote Sensing,
Tibet University,
Lhasa, 850000, China
Email: chennsh@imde.ac.cn

Z. Zhong
Kunming University of Science and Technology,
Kunming, 650504, China

M. Rahman
Department of Civil Engineering,
International University of Business Agriculture and Technology (IUBAT),
Dhaka, 1230, Bangladesh